Influence of ZrO$_2$ Nanoparticles on the Microstructural Development of Cement Mortars with Limestone Aggregates

Danna L. Trejo-Arroyo [1],*, Karen E. Acosta [2], Julio C. Cruz [2], Ana M. Valenzuela-Muñiz [3], Ricardo E. Vega-Azamar [2] and Luis F. Jiménez [2]

[1] CONACYT-Tecnológico Nacional de México/I.T. Chetumal; Insurgentes 330, Chetumal 77050, QR, Mexico
[2] Tecnológico Nacional de México/I.T. Chetumal; Insurgentes 330, Chetumal 77050, QR, Mexico; M10390091@itchetumal.edu.mx (K.E.A.); jcruz@itchetumal.edu.mx (J.C.C.); revega@itchetumal.edu.mx (R.E.V.-A.); fjtorrez@itchetumal.edu.mx (L.F.J.)
[3] CONACYT-Tecnológico Nacional de México/I.T. Cancún; Kabah Km 3, Cancún 77515, QR, México; amvalenzuelamu@conacyt.mx
* Correspondence: dltrejoar@conacyt.mx; Tel.: +52(983)8321019 (ext. 147)

check for updates

Abstract: In this research, the effect of the addition of zirconium oxide-synthesized nanoparticles on the microstructural development and the physical–mechanical properties of cement mortars with limestone aggregates was studied. Zirconia nanoparticles were synthesized using the co-precipitation method. According to XRD analysis, a mixture of tetragonal (t) and monoclinic (m) zirconia phases was obtained, with average crystallite sizes around 15.18 and 17.79 nm, respectively. Based on the ASTM standards, a mixture design was obtained for a coating mortar with a final sand/cement ratio of 1:2.78 and a water/cement ratio of 0.58. Control mortars and mortars with ZrO$_2$ additions were analyzed for two stages of curing of the mortar—7 and 28 days. According to SEM analysis, mortars with ZrO$_2$ revealed a microstructure with a high compaction degree and an increase in compressive strength of 9% on the control mortars. Due to the aggregates' characteristics, adherence with the cement paste in the interface zone was increased. It is suggested that the reinforcing effect of ZrO$_2$ on the mortars was caused by the effect of nucleation sites in the main phase C–S–H and the inhibition of the growth of large CH crystals, and the filler effect generated by the nanometric size of the particles. This produced a greater compaction volume, suggesting that faults are probably originated in the aggregates.

Keywords: zirconium oxide nanoparticles; microstructure; limestone aggregates; cementitious composites

1. Introduction

Mortars and concretes are cementitious composites whose physical and mechanical properties are affected by each material in their constitution, such as the cementing agent, the fine and/or coarse aggregates, and the water. In the construction industry, mortar is the mixture of the raw materials, the binder component such as cement or lime, water, and sand, which form a paste that hardens during the process and hydration kinetics. It is essential to know the components and the characteristics of each element, such as the type and content of sand or fine aggregates, since these physical or chemical characteristics modify, in a different way, the structure of the mixture from workability to performance in the use phase [1]. The sand, or fine aggregate, used for the manufacture of mortars, can come from different sources, such as natural deposits (called natural sand or siliceous sand) or as crushed rock products (like limestone aggregates), each of them having distinctive physical characteristics that influence mortars and concretes differently [2,3]. When it comes to concrete, the mixture volume

depends on size distribution and aggregate shape. The most important factor determining the water amount needed is the aggregate shape and its surface characteristics—the greater the surface area, the higher the water demand [4,5]. On their part, limestone aggregates have certain characteristics, such as rough surface texture and irregular shape, which favors the increment of adhesion between the cement paste and the aggregates [6]. The chemical interaction between limestone aggregate and cementing matrix produces an increase in the strength bond among them at older ages in the area known as interface zone [7], which is considered the weakest component [8]. This reaction also favors the mixture compressive strength, depending mainly on the aggregate density. However, due to the high porosity and low resistance that crushed limestone aggregates present, in practice, cement demand is increased so that the design resistances can be reached [2,4]. The mortar is moldable in a fresh state and, once hardened, it obtains characteristics such as strength, durability, and adhesion [9]. These characteristics are affected by aggressive agents such as humidity, salinity, and the extreme temperatures of subhumid warm regions, as well as by the mortar components themselves. As a consequence, porosity increases, structure weakens, and mortar cracking and detachment occurs. However, mortars and concretes may be modified with commercial or alternative additives, which modify a particular physical property of the mixture, allowing the transformation and/or modification of certain properties of a product during mixing or in its final stage [10].

The construction industry has considered the implementation of nanomaterials as an alternative solution for several problems. For the development of cementitious composites with structural properties presenting better mechanical performances or multifunctional properties, it is necessary to carry out the manipulation of the structure at the micro and nanometric scale [11]. Measurements and characterization, performed at the mentioned scale of cement-based materials, allows a better understanding of the material behavior at the macroscopic scale [12]. In the last years, several investigations about the use of nanoparticles have been developed to improve the physical, mechanical, and/or functional properties of already existing materials, with an improvement projection including efficiency, resistance, and durability of cementing pastes, as well as their sustainability [13–15].

Nanoparticles can significantly modify the mechanical properties and the microstructure of cementitious composites due to their high surface areas and high activity [15]. Zirconium oxide is a non-reactive ceramic material with a wide range of applications due to its unique combination of physical–chemical and mechanical properties, such as high corrosion resistance, low thermal conductivity and insulating properties, high strength, and excellent fracture toughness [14,15]. Its properties depend on its crystalline structure and on the phase transformations to which it is subjected, being a great alternative as a reinforcing material for cementitious composites such as mortars and/or concretes [16]. In the literature, it has been reported that ordinary Portland cement (OPC) with partial replacement of zirconium oxide nanoparticles significantly increase the values of split tensile strength, flexural strength, and strength of concrete due to the rapid consumption of $Ca(OH)_2$ and release from cement hydration, which is related to the high reactivity of the zirconia particles. Therefore, the hydration of cement is accelerated; generating large volumes of hydration products, increasing the packing density of the cement particles and reducing the volume of large pores in the cementing paste [17,18]. It has also been found that the increase in the percent volume fraction of zirconium oxide nanoparticles decreases the initial and final setting time of the concretes, indicating that zirconium oxide nanoparticles have a higher hydration reaction rate than cement, since they are characterized by unique surface effects, smaller particle sizes, and higher surface energy [18,19]. It has also been reported that the workability of mortar or concrete mixtures decreases with the increasing of zirconium oxide nanoparticle content [20]. With smaller particle sizes and surface area, water demand increases. If the water-to-cement ratio remains constant, and the volume fraction of zirconium oxide nanoparticles increases, the workability of the fresh concrete is diminished. It has been reported that the optimal value of zirconium oxide nanoparticles as partial substitute for cement is 1% by weight of cement [18]. With 1% of zirconium oxide nanoparticles, pore distribution is refined and porosity decreases, compared to cementitious pastes without nanoparticles. The effect of zirconium oxide nanoparticles on the

mechanical and thermal properties of cement aluminate-based pastes has also been stated in the literature [21]; for thermal energy-storing materials, it has been determined that the optimum value of zirconium oxide nanoparticle addition is 1% by weight, reaching the best results in the properties. Similarly, thermal conductivity and volumetric heat capacity of pastes enriched with zirconium oxide nanoparticles were improved. Zirconium oxide nanoparticles have also been added in reactive powder concretes (RPC); several works showed that zirconium oxide nanoparticles do not accelerate the hydration process of RPCs, however, they can make the hydration products distribution more uniform, restricting the growth space of CH crystals, obtaining denser microstructures of these concretes. It has also been reported that high contents of zirconium oxide nanoparticles can contribute to better mechanical properties (up to 3% by weight), however, in the absence of a good dispersion, they can agglomerate and weaken the reinforcing effect [22,23].

Most of the works presented in the literature regarding mortars or concretes have focused on the development and optimization of mechanical properties as a function of curing time, different curing media, and/or percentage of nanoparticle addition. They establish the fine aggregates (natural sand, river sand, or silica sand), cement, and water as part of the composite matrix, where the characteristics in the resistance values and the developed microstructure are not related as a function of the aggregate type or sand. With the addition of zirconium oxide nanoparticles, which is one of the least reported nanoparticles in the literature for similar research, these characteristics may be influenced by the different composites matrices. In general, any mortar or concrete may be improved in its physical properties and resistance with the addition of certain types of nanoparticles, however, the aforementioned becomes more relevant for the case of those elaborated with crushed limestone aggregates, due to their surface characteristics, such as roughness, texture, and porosity, which make the mixture absorb more water, increasing the cement demand to reach the design resistance. Therefore, globally, the potential impact of nanoparticle-added mortars, such as that in the present work, is the reduction of the amount of cement used in the mix, which entails both a lower production cost and a lower carbon footprint. Therefore, the objective of this study was to investigate the effect of zirconium oxide nanoparticles, cement, and limestone aggregates, characteristic of warm subhumid coastal regions (in the Southeast of Mexico), on several properties, such as the physical properties and compressive strength of cement-based cementitious composites as a function of microstructural development.

2. Materials and Methods

2.1. Synthesis and Characterization of ZrO_2 Nanoparticles

Zirconium oxide nanoparticles (ZrO_2) were synthesized according to the literature by the co-precipitation method [24–26], using octahydrate zirconium chloride (Sigma-Aldrich, 98% purity, Saint Louis, MO, USA) doped at 7.5% mol of $YO_{1.5}$, yttrium chloride, anhydrous, YCl3 (Sigma-Aldrich,, 99.9% purity, Saint Louis, MO, USA) as precursor salt, and ammonium hydroxide NH_4OH as a precipitant. Each precursor salt was dissolved separately in deionized water with constant agitation for 30 min, and then they were mixed with continuous stirring for another 30 min. Subsequently, ammonium hydroxide 25 wt % was added. The pH of the solution was maintained ~9; the addition of this was done drop by drop, to avoid a strong agglomeration in the solution. After precipitation, the slurry was stirred for another 30 min and then heated at 80 °C for a certain time under continuous stirring. The resultant gel was filtered, and then washed with deionized water until no Cl^- was detected. The obtained powders were calcinated at 500 °C for 1 hour, according to the equilibrium phase diagram of ZrO_2–$YO_{1.5}$ [16]. Samples were analyzed by X-ray diffraction (Bruker AXS D8 Advance, diffractometer, at a voltage of 40 kV, current of 40 mA and using Cu Kα radiation with a wavelength of 1.54 Å, Cancun, QR, Mexico) to determine the present phases, and crystallite size was calculated using the D. Scherrer formula from the peak intensities of the X-ray diffraction (XRD) patterns [27].

The morphological analysis was carried out by scanning electron microscopy (SEM) in a JEOL JSM-6010PLUS/LA microscope, (Chetumal, QR, Mexico), equipped with energy dispersive X-ray spectroscopy (EDX).

2.2. Limestone Fine Aggregate

The cementing material was ordinary Portland cement, OPC. The sand used for this study was a fine aggregate obtained from the crushing of locally available limestone. In addition, a series of tests was conducted for the fine aggregates to evaluate the basic physical properties. For the granulometry tests, it was determined that the samples fulfilled the lower percentage between 2 consecutive meshes as indicated by the ASTM C136 standard [28], that is, not exceeding 50% of the material. Fine aggregates were characterized by grain size, according to ASTM C144 standard [29], specific gravity, and absorption, according to ASTM C128 standard [30], to obtain the data necessary for the mix design.

Due to the type of the limestone fine aggregate used, a mixture adjustment was performed, setting the final proportions of cement/fine aggregate at 1:2.78 and a water/cement ratio of 0.58.

Morphological analysis and semi-quantitative elemental chemical analysis were obtained by scanning electron microscopy (SEM) and energy dispersive X-ray spectroscopy (EDX), respectively.

2.3. Cementitious Composites (Mortars)

Once the fine limestone aggregates were characterized, the samples of mortar were prepared. Reference mortar samples (RM) with 0% of ZrO_2 nanoparticle addition and samples with 1% weight of ZrO_2 nanoparticles (ZM) as a partial cement substitute were made. The analysis of the physical properties, such as density, percentage of absorption, and pore percentage, were carried out based on the ASTM C 642 [31] standard at 7 and 28 days of curing in water. To obtain valid statistical results, 10 cylindrical mortar specimens were made for each composition with dimensions of 2" diameter by 40 mm high. The compressive strength test was carried out according to the ASTM C 109 [32] standard. Based on this, groups of 6 specimens of each mortar were made in cubic molds of 5 cm edge.

For the microstructural analysis, by SEM, samples of RM and ZM were extracted from the fractured cubes that were subjected to compression.

3. Results

3.1. Characterization of Fine Aggregates

Figure 1a shows a SEM image of the limestone aggregates passing the 200 mesh (74 μm), where the general physical aspect is observed, like their irregular shapes of angular type and a narrow size distribution. Figure 1b shows the detailed particle size distributions of the fine limestone aggregates obtained by sieving. The gradation curve shows a slight deficiency in the particle size distribution; however, this sand was used trying to have results as close as possible to actual working conditions for the fine finishing mortar, which has a fineness modulus of 2.63, a percentage of absorption of 5.1, and a specific gravity of 2.5. The summary of the physical properties is listed in Table 1.

Figure 1a shows a SEM image of the limestone aggregates that pass the 200 mesh (74 μm), where the general physical aspect is observed, like their irregular shapes and with a narrow size distribution. Figure 1b shows the limestone aggregates granulometry and it depicts the deficiencies in the particle size distribution; however, this sand was used in an attempt to produce results as close as possible to actual working conditions for the fine finishing mortar, which has a fineness modulus of 2.63.
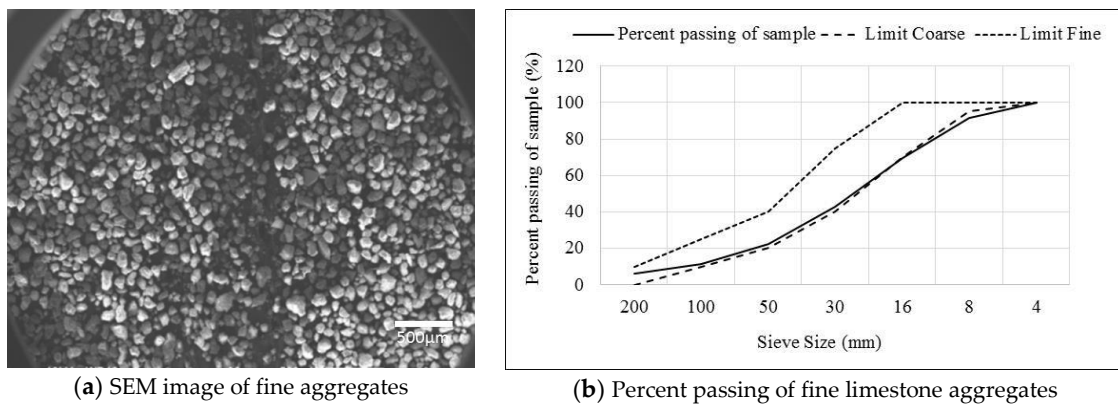
(**a**) SEM image of fine aggregates

(**b**) Percent passing of fine limestone aggregates

Figure 1. Micrograph obtained by SEM of aggregates passing the 200 mesh and granulometric curve of the fine limestone aggregates with a fineness modulus of 2.63.

Table 1. Physical properties of limestone aggregates.

Sample	Absorption (%)	Fineness modulus	Specific gravity
Average	5.1	2.63	2.5

In Figure 2, an image from a particle of the aggregates is observed as well as the result of the elemental chemical composition by EDX. Figure 2a shows a fracture surface that presents diverse flat and cleaved surfaces along the planes, and structures in the shape of polyhedrons with well-defined corners that form the particles. Several EDX analyzes were performed per sample. Results indicated that the limestone aggregates contained a high magnesium percentage (Mg) as shown in Figure 2b. According to the literature [7,33,34], this could correspond to a type of aggregate not clastic, coming from sedimentary crushed rocks called dolomite.Therefore, it is a carbonate mineral (calcium magnesium carbonate, $CaMg(CO_3)_2$) formed by chemical or biological precipitations from seawater reacting with $CaCO_3$, whose main components are calcite and dolomite.
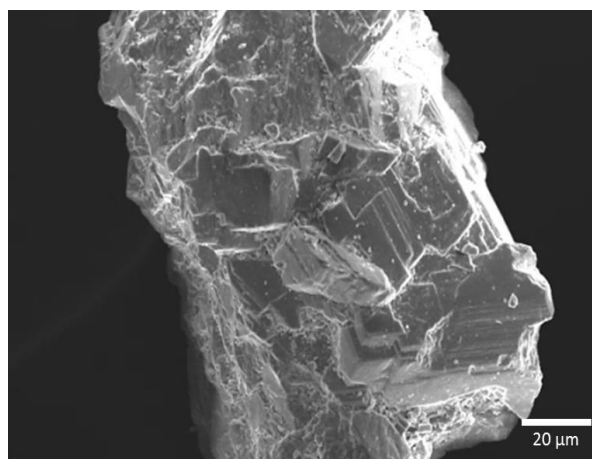
(**a**) SEM of a limestone aggregate particle

Formula	Mass %	Atom %
O	47.48	61.78
Mg	32.49	27.82
Ca	20.04	10.41
Total	100	100

(**b**) Elemental chemical analysis

Figure 2. Micrograph obtained by SEM of a limestone aggregate particle and its elemental chemical analysis carried out by EDX.

The X-ray diffraction analysis of the aggregates shows that the characteristic peaks corresponded to the crystalline structure of calcite and dolomite, as is possible to observe in Figure 3. The results corroborate that the fine aggregates used for the preparation of mortars for this investigation correspond to calcitic dolomitic.
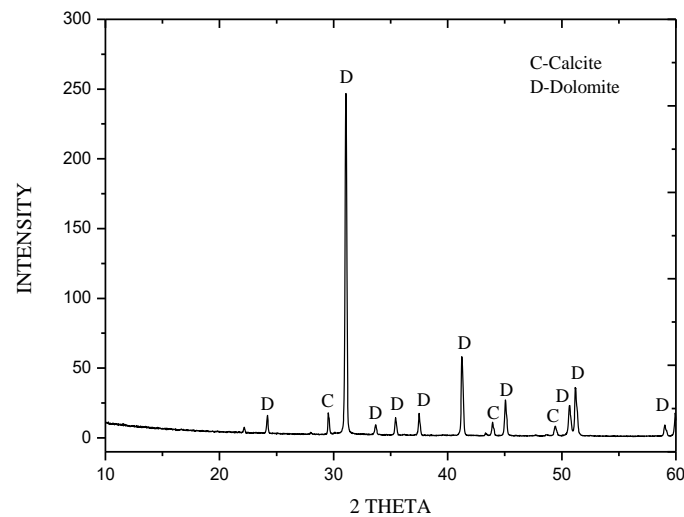
Figure 3. X-ray diffraction pattern of fine limestone aggregates.

3.2. X-Ray Diffraction of Zirconia Nanoparticles

Figure 4 shows the XRD pattern of zirconia-synthesized powders, in which the characteristic peaks of the tetragonal (t) and monoclinic (m) phase of zirconia are presented. According to Scherrer equation [24], the estimated crystallite size corresponds to 15.18 and 17.79 nm, respectively. Reflection of the sample is relatively broad, indicating that the sample consists of amorphous phase. It could be a pseudocrystalline phase due to the low calcination temperature, since it has been reported that the amorphous phase decreases gradually with the increase of calcination temperature and disappears when calcined at 800 °C [23]. With the increase in temperature, shrinkage increases in the peaks, indicating an increase in the degree of crystallinity and the growth of the crystal size at higher temperatures.
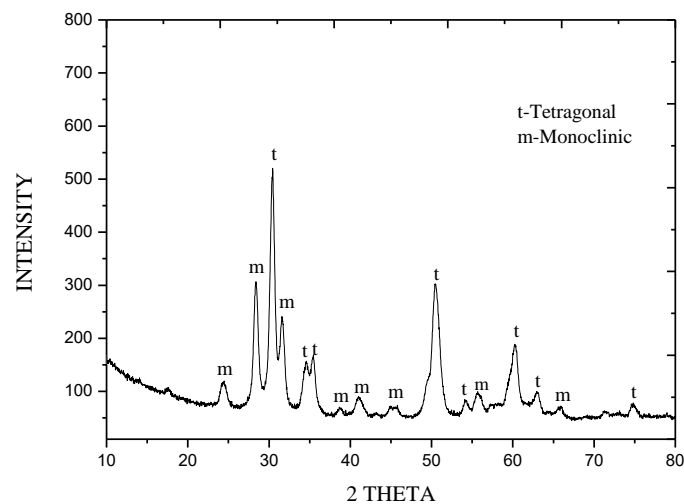

Figure 4. X-ray diffraction pattern of zirconia-synthesized powders calcined at 500 °C/1 h.

3.3. Physical–Mechanical Characterization of Cementitious Composites (Mortars)

The samples of mortar with ZrO_2 nanoparticles, ZM, exhibited different results in their physical properties when compared to the reference mortars, RM, as shown in Figure 5. Apparent density of ZM after 7 days of curing reached 2.66 g/cm^3 with 35.8% of permeable pore volume while, at 28 days, it reached its maximum of 2.71 g/cm^3. Apparent density of RM was 2.45 and 2.52 g/cm^3 at 7 and 28 days respectively, with a permeable space volume of 36.6%.
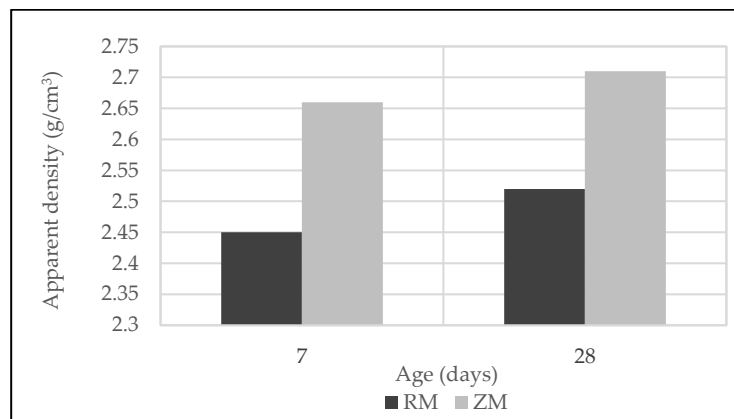
Figure 5. Apparent density of mortars with ZrO_2 nanoparticles additions and reference mortars.

Regarding the compressive strength of RM and ZM mortars, results for 7 and 28 days of curing are shown in the graph of Figure 6. At 7 days, ZM mortars showed greater resistances than those of RM mortars. Following the same trend, after 28 days, compressive strength of ZM mortars surpassed the values of reference mortars.
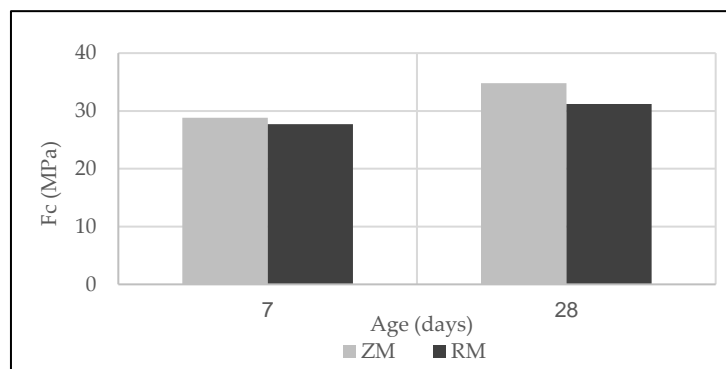

Figure 6. Compressive strength of mortars with ZrO_2 nanoparticle additions and reference mortars.

3.4. Microstructural Characterization of Cementitious Composites (Mortars)

As for SEM, the microstructural development analysis of reference mortars and of those with ZrO_2 nanoparticle addition was carried out after 28 days of curing. The image in Figure 7 corresponds to micrographs of the surface of fractured mortars at a magnification of $100\times$. Reference mortar corresponds to Figure 7a, where a high percentage of voids (or holes) generated during cement hydration, oscillating around 20 to 250 μm, can be observed; the large reliefs shown in the image may correspond to the specimen fracture behavior. Figure 7b corresponds to the ZrO_2 nanoparticle-added mortar where large voids or holes are not observed, although there is a considerable porosity appearance.

(**a**) Reference mortar   (**b**) Mortar with ZrO_2 nanoparticle addition.
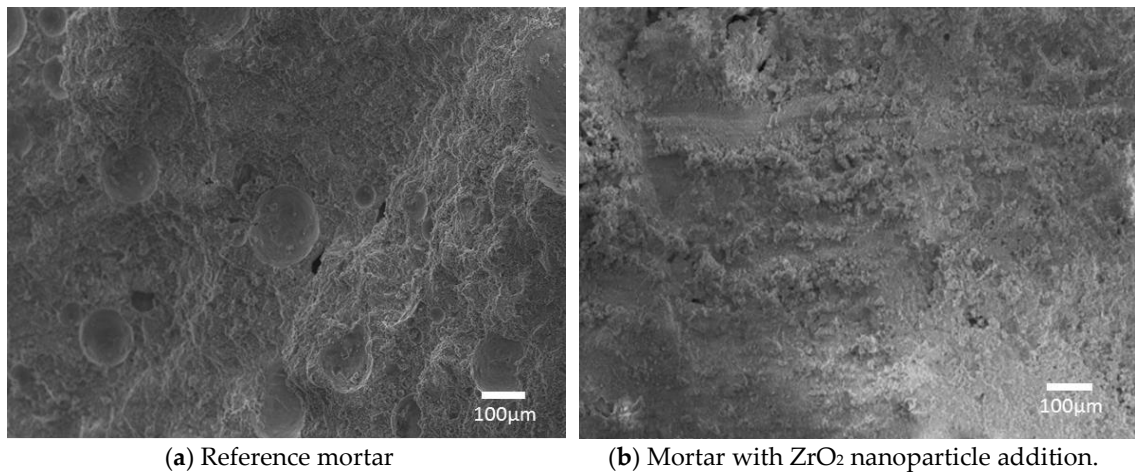
Figure 7. SEM of mortar fracture surface after 28 days of curing.

Figure 8 shows micrographs corresponding to RM at higher magnifications. In Figure 8a, the distinctive microstructural characteristics of hydrated cement can be observed, such as the tobermorite gel phase (C–S–H), which is the non-crystalline phase overlapped, or joined, around some limestone aggregates grains, some of them fractured [35]. The generation of ettringite crystals can be noticed in the interface zone between the tobermorite and the aggregate, at the edges, and at the center of holes. Large portlandite crystals (Ca(OH)$_2$), with sizes around 5 µm, can also be noted clearly seen in the micrograph in Figure 8b, which corresponds to a magnification in the vicinity of the gap. The tobermorite phase can also be observed, some portlandite crystals distributed between the specimen and areas with intertwined crystals in the form of small needles corresponding to ettringite crystals.
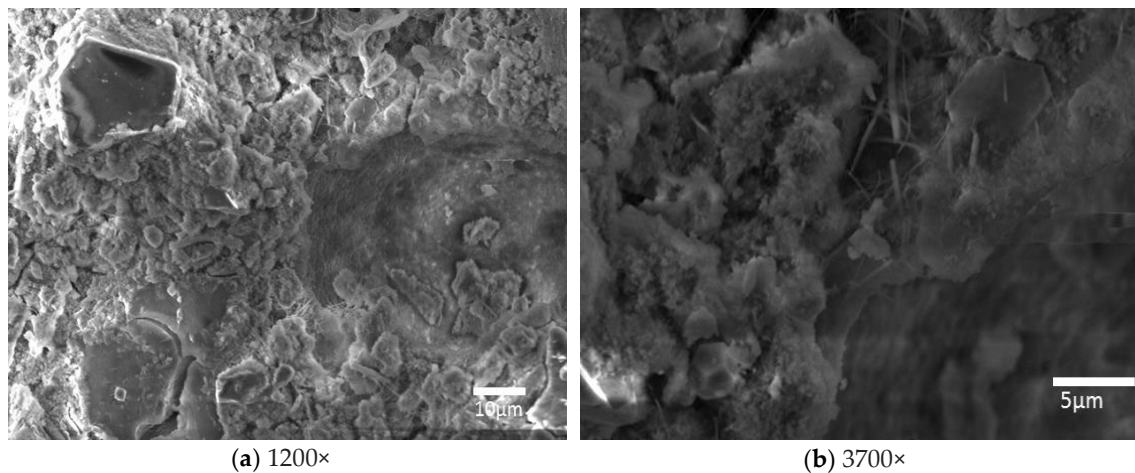

(**a**) 1200×   (**b**) 3700×

Figure 8. SEM of the fracture surface in the reference mortar.

The microstructure of mortars with ZrO_2 nanoparticles added is shown in Figure 9a, where can be observed that the development of hydration products was more compact, compared to the reference mortars. It is possible to note the particular relief generated by the type of fracture of the cementing material, formed by a set of aggregates with well-defined borders, completely adhered to the cementing paste. It can be noticed how this cementing paste covers the set of limestone aggregates achieving a high adherence between their surfaces, as shown in Figure 9b, which corresponds to higher magnifications. For its part, the contribution of zirconia particles in the level of compaction of the composite may be due to their effect as preferred nucleation sites for the formation of cement hydration products generated by them due to their high surface energy, as has been mentioned in the literature. A high degree of compaction is observed between the aggregates with cleaved regions along

the planesandpreferred directions producing flat surfaces. It is presumed that his behavior occurred due to a mechanical effect to which it was exposed.
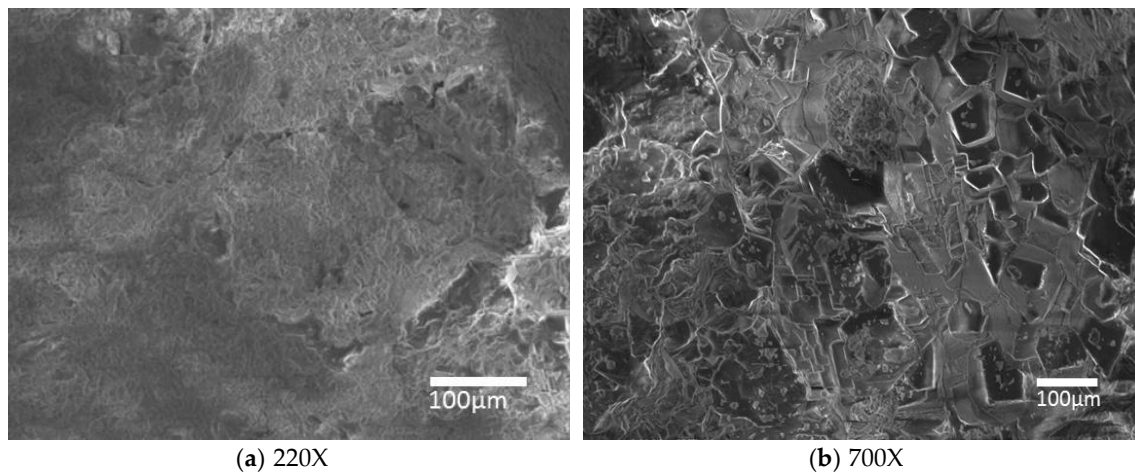

(**a**) 220X   (**b**) 700X

Figure 9. SEM micrographs of the fracture surface of ZrO_2 nanoparticle-added mortars cured at 28 days.

4. Discussion

Zirconia particles in tetragonal and monoclinic phases with submicronic particle sizes with crystallite sizes of 15.18 and 17.79 nm, respectively, were synthesized by coprecipitation of zirconia nanoparticles doped at 7.5 mol% with $YO_{1.5}$.

Cement mortars with addition of these synthesized particles presented a microstructural development with a greater compaction degree than the reference mortars, smaller volume of pore space, and higher compressive strength, which allows inferring a good surface activity due to the high surface area of the obtained particles.

The efficiency of ZrO_2 nanoparticles, in terms of the increase in resistance, was around 19%, possibly due to nanoparticle surface effects, which have a faster reaction rate than that of cement and may influence compressive strength at both ages. In addition, limestone aggregates have irregular shapes, rough texture, and they react or produce greater bonding between the aggregate particles and cement paste; there is an increment in the adhesion strength that can be correlated to a greater resistance [3]. Additionally, in the literature [16], it has been reported that phase transformation effect occurs when zirconia in tetragonal phase is subjected to mechanical stresses and undergoes a martensitic transformation to the monoclinic phase, which involves an increase in volume of approximately 4%, which should contribute to the inhibition of the growth of cracks and the increase of compressive strength [24]. However, more studies will have to be carried out to identify and isolate the mentioned reinforcement mechanism in the matrix of the cementitious composite. According to the literature, since ZrO_2 nanoparticles are characterized by their particle sizes with greater surface area, they increase the packing density of the cement particles, reducing the volume of permeable pores in the mixtures [18].

According to SEM analysis, the reference mortars made with limestone aggregates presented a microporosity ranging from 10 nm to 1 μm, which depends mainly on the hydration degree, and they also presented a macroporosity consisting of entrained air in the form of spherical bubbles and sizes between 20 and 200 μm, besides the aggregate's porosity, that can greatly influence the properties of the mortar [36]. According to the literature [37], pores smaller than 1 μm contribute to the transfer of capillary water while, in finer pores, the water is bound to the material and these pores do not contribute to water transfer. Pores greater than 100 μm can contribute to water permeability by gravity or to the entry of water driven by the wind.

The exposure of mortars on exposed surfaces in coastal areas is subject to high environmental loads, such as a high degree of salinity, high relative humidity, and high temperatures for most of the year. The soluble salts in mortars, supplied from external sources, may present a serious risk for their durability. Salts may come from the raw material or be supplied from external sources, such as the salt-laden wind and salt from the soil and groundwater that is transported through the walls or from wastes. Therefore, a low percentage of permeable pores in the mortars is required.

It is suggested that the type, form, and composition of the aggregate (dolomitic limestone) contribute, to a certain extent, to the microstructural development of mortars and also to the physical–mechanical behavior. In the reference mortars, these characteristics increase the adhesion with the cement paste and decrease the porosity in the interface zone, generating a greater compaction volume, which implies that faults may be originated in the aggregates. In the zirconia-added mortars, SEM images showed that aggregates tend to cleave along the planes, producing flat surfaces.

5. Conclusions

The microstructural development of cementitious composites with limestone aggregates and the addition of zirconia nanoparticles as a means of reinforcement was evaluated in mortars, in relation to their physical properties and compressive strength.

It was found that type, shape, and composition of the aggregate contribute to the microstructural development of cement mortars. In mortars with limestone aggregates, the analysis suggests that the failure onset originates within the aggregates and not in the interfacial zone.

In the zirconia-added mortars, a less porous microstructure was developed with a greater degree of compaction, which is reflected in an increase in the density and the compressive strength.

The analysis carried out in the work suggests that the reinforcement of the added mortars is due to the high surface activity of the zirconia nanoparticles. Reinforcement in the zirconia-added mortars is derived mainly from three mechanisms: the filler effect, nucleation effect, and the phase transformation effect. The filler effect is exerted by zirconia particles when they are trapped in the empty spaces, or pores, generated by the cement's own hydration process, resulting in the filling of the interstices. Regarding the nucleation effect, zirconia particles serve as preferential nucleation sites for cement hydration products, either within the pore space or at the interface between the cement paste and the aggregates, or between the hydration products, generating a higher (CSH) tobermorite phase content and inhibiting the growth of calcium hydroxide crystals $Ca(OH)_2$.

In spite of all of the above, more research is required using specific techniques to analyze the reinforcement mechanism exerted by the zirconia particles on the matrix of the composite. A high void content was not observed in the aggregates, taking into account that the absorption percentage is a proxy of the void content, which was also corroborated by SEM.

The use of zirconia nanoparticles in cementitious composites with limestone aggregates has produced microstructural development with a direct benefit in the reinforcement of the matrix, which generates an important incentive for a research avenue of a greater scope, leading to better development of the mechanical properties through microstructural control.

References

1. Yaşar, E.; Erdoğan, Y.; Kılıç, A. Effect of limestone aggregate type and water–cement ratio on concrete strength. *Mater. Lett.* **2004**, *58*, 772–777. [CrossRef]
2. Chan, J.L.; Solís, R.; Moreno, E.I. Influencia de los agregados pétreos en las características del concreto. *Ingeniería* **2003**, *7*, 39–46.
3. Adams, M.P.; Ideker, J.H. Influence of aggregate type on conversion and strength in calcium aluminate. *Cem. Concr. Res.* **2017**, *100*, 284–296. [CrossRef]
4. Huang, Y.; Wang, L. Effect of particle shape of limestone manufactured sand and natural sand on concrete. *Procedia Eng.* **2017**, *210*, 87–92. [CrossRef]
5. Chen, X.; Wu, S.; Zhou, J. Pore size distribution of cement mortar prepared with crushed limestone sand. *KSCE J. Civ. Eng.* **2017**, *20*, 762–767. [CrossRef]
6. An, J.; Kim, S.S.; Nam, B.H.; Durham, S.A. Effect of aggregate mineralogy and concrete microstructure on thermal expansion and strength properties of concrete. *Appl. Sci.* **2017**, *7*, 1307. [CrossRef]
7. Tasong, W.A.; Lynsdale, C.J.; Cripps, J.C. Aggregate-cement paste interface, Part I; Influence of aggregate geochemistry. *Cem. Concr. Res.* **1999**, *29*, 1019–1025. [CrossRef]
8. Jebli, M.; Jamin, F.; Malachanne, E.; Garcia-Diaz, E.; El Youssoufi, M.S. Experimental characterization of mechanical properties of the cement-aggregate interface in concrete. *Constr. Build. Mater.* **2018**, *161*, 16–25. [CrossRef]
9. CONCRETE: Microstructure, Properties and Materials. Available online: http://103.248.208.114:8080/dspace/bitstream/123456789/515/1/book.pdf (accessed on 6 February 2019).
10. Monteiro, K.M. Concreto, estructura, propiedades y materiales, IMCYC. 1ª edición IMCYC, México D.F., México. 1998.
11. Singh, N.B.; Kalra, M.; Saxena, S.K. Nanoscience of cement and concrete. *Mater. Today: Proc.* **2017**, *4*, 5478–5487. [CrossRef]
12. Pacheco-Torgal, F.; Jalali, S. Nanotechnology: Advantages and drawbacks in the field of construction and building materials. *Constr. Build. Mater.* **2011**, *25*, 582–590. [CrossRef]
13. Sanchez, F.; Sobolev, K. Nanotechnology in concrete—A review. *Constr. Build. Mater.* **2010**, *24*, 2060–2071. [CrossRef]
14. Norhasri, M.S.M.; Hamidah, M.S.; Fadzil, A.M. Applications of using nano material in concrete: A review. *Constr. Build. Mater.* **2017**, *133*, 91–97. [CrossRef]
15. Rashad, A.M. Effects of ZnO_2, ZrO_2, Cu_2O_3, CuO, $CaCO_3$, SF, FA, cement and geothermal silica waste nanoparticles on properties of cementitious materials—A short guide for Civil Engineer. *Constr. Build. Mater.* **2013**, *48*, 1120–1133. [CrossRef]
16. Hannink, R.H.J.; Kelly, P.M.; Muddle, B.C. Transformation toughening in zirconia-containing ceramics. *J. Am. Ceram. Soc.* **2000**, *83*, 461–487. [CrossRef]
17. Nazari, A.; Shadi, R.; Shirin, R.; Shamekhi, S.F.; Khademno, A. Embedded ZrO_2 nanoparticles mechanical properties monitoring in cementitious composites. *J. Am. Sci.* **2010**, *6*, 86–89.
18. Negahdary, M.; Habibi-Tamijani, A.; Asadi, A.; Ayati, S. Synthesis of zirconia nanoparticles and their ameliorative roles as additives concrete structures. *J. Chem.* **2012**, *2013*. [CrossRef]
19. Rafieipour, M.H.; Nazari, A.; Mohandesi, M.A.; Khalaj, G. Improvement compressive strength of cementitious composites in different curing media by incorporating ZrO_2 nanoparticles. *Mat. Res.* **2012**, *15*, 177–184. [CrossRef]
20. Nazari, A.; Riahi, S.; Riahi, S.; Shamekhi, S.F.; Khademno, A. An investigation on the Strength and workability of cement based concrete performance by using ZrO_2 nanoparticles. *J. Am. Sci.* **2010**, *6*, 29–33.
21. Yuan, H.; Shi, Y.; Xu, Z.; Lu, C.; Ni, Y.; Lan, X. Influence of nano-ZrO_2 on the mechanical and thermal properties of high temperature cementitious thermal energy storage materials. *Constr. Build. Mater.* **2013**, *48*, 6–10. [CrossRef]
22. Han, B.; Wang, Z.; Zeng, S.; Zhou, D.; Yu, X.; Cui, X.; Ou, J. Properties and modification mechanisms of nano-zirconia filled reactive powder concrete. *Constr. Build. Mater.* **2017**, *141*, 426–434. [CrossRef]
23. Ruan, Y.; Han, B.; Yu, X.; Li, Z.; Wang, J.; Dong, S.; Ou, J. Mechanical behaviors of nano-zirconia reinforced reactive powder. *Constr. Build. Mater.* **2018**, *162*, 663–673.

24. Fei, L.; Yanhuai, L.; Zhongxiao, S.; Kewei, X.; Zhi, Z.; Hong, C. Rietveld study on evolution of crystalline structure of ysz nanoparticles during co-precipitation synthesis. *Rare Metal Mat. Eng.* **2015**, *44*, 2716–2720. [CrossRef]

25. Rezaei, M.S.; Alavi, M.S.; Sahebdelfar, S.; Yan, Z.; Teunissen, H.; Jacobsen, J.H.; Sehested, J. Synthesis of pure tetragonal zirconium oxide with high surface area. *J. Matter Sci.* **2007**, *42*, 1228–1237. [CrossRef]

26. Viazzi, C.; Bonino, J.P.; Ansart, F.; Barnabé, A. Structural study of metastable tetragonal YSZ powders produced via a sol–gel route. *J. Alloys Compd.* **2008**, *452*, 377–383. [CrossRef]

27. Monshi, A.; Foroughi, M.R.; Monshi, M.R. Modified scherrer equation to estimate more accurately nano-crystallite size using XRD. *Word J. Nano Sci. Eng.* **2012**, *2*, 154–160. [CrossRef]

28. ASTM International. Standard Test Method for Sieve Analysis of Fine and Coarse Aggregates. In *Annual Book of ASTM Standards*; ASTM C136–06; American Society for Testing and Materials: West Conshohocken, PA, USA, 2006.

29. ASTM International. Standard Specification for Aggregate for Masonry Mortar. In *Annual Book of ASTM Standards*; ASTM C144–11; American Society for Testing and Materials: West Conshohocken, PA, USA, 2011.

30. ASTM International. Standard Test Method for Relative Density (Specific Gravity) and Absorption of Fine Aggregate. In *Annual Book of ASTM Standards*; ASTM C128-15; American Society for Testing and Materials: West Conshohocken, PA, USA, 2015.

31. ASTM International. Standard Test Method for Density, Absorption, and Voids in Hardened Concrete. In *Annual Book of ASTM Standards*; ASTM C 642-13; American Society for Testing and Materials: West Conshohocken, PA, USA, 2013.

32. ASTM International. Standard Test Method for Compressive Strength of Hydraulic Cement Mortars (Using 2-in. or [50-mm] Cube Specimens). In *Annual Book of ASTM Standards*; ASTM C109/C109M-16a; American Society for Testing and Materials: West Conshohocken, PA, USA, 2016.

33. Jiménez, L.F.; Domínguez, J.A.; Vega-Azamar, R.E. Carbon Footprint of Recycled Aggregate Concrete. *Adv. Civ. Eng.* **2018**, *2018*, 6. [CrossRef]

34. Walther, J. *Essentials of Geochemistry*; Jones & Bartlett Learning: Sudbury, MA, USA, 2009.

35. Bullard, J.W.; Jennings, H.M.; Livingston, R.A.; Nonat, A.; Schereri, G.W.; Schweitzer, J.S.; Scrivener, K.L.; Thomas, J.J. Mechanisms of cement hydration. *Cem. Concr. Res.* **2011**, *41*, 1208–1223. [CrossRef]

36. Giosuè, C.; Pierpaoli, M.; Mobili, A.; Ruello, M.L.; Tittarelli, F. Influence of binders and lightweight aggregates on the properties of cementitious mortars: From traditional requirements to indoor air quality improvement. *Materials* **2017**, *10*, 978. [CrossRef]

37. Characterisation of old mortars with respect to their repair; Chapter: 2.5. Available online: https://www.researchgate.net/profile/Caspar_Groot/publication/319470227_Chapter_25_Characterisation_Porosity_of_mortars/links/59ad817faca272f8a1617e8a/Chapter-25-Characterisation-Porosity-of-mortars.pdf (accessed on 6 February 2019).